ScientificScholar®
Knowledge is power
Publisher of Scientific Journals

www.clinicalimagingscience.org

Journal of Clinical Imaging Science

Neuroradiology/Head and Neck Imaging *Original Research*

Unruptured Arteriovenous Malformations in the Multidetector Computed Tomography Era: Frequency of Detection and Predictable Failures

Raghav R. Mattay[1], Lane Miner[2], Alexander Z. Copelan[3], Karapet Davtyan[1], James E. Schmitt[1], Ephraim W. Church[4], Alexander C. Mamourian[2]

[1]Department of Radiology, Hospital of the University of Pennsylvania, Philadelphia, [2]Department of Radiology, Penn State Milton S. Hershey Medical Center, Hershey, Pennsylvania, [3]Department of Interventional Neuroradiology, Abbot Northwestern Hospital Neuroscience Institute, Minneapolis, Minnesota, [4]Department of Neurosurgery, Penn State Milton S. Hershey Medical Center, Hershey, Pennsylvania, United States.

***Corresponding author:**
Raghav R Mattay,
Department of Radiology,
Hospital of the University of Pennsylvania, Philadelphia, Pennsylvania, United States.

rrmattay@gmail.com

Received : 04 November 2021
Accepted : 12 January 2022
Published : 18 February 2022

DOI
10.25259/JCIS_200_2021

Quick Response Code:

ABSTRACT

Objectives: While hemorrhage arising from ruptured arteriovenous malformations (AVMs) is usually evident on multidetector non-contrast computed tomography (NCCT), unruptured AVMs can be below the limits of detection. We performed a retrospective review of NCCT of patients with a proven diagnosis of unruptured AVM to determine if advances in CT technology have made them more apparent and what features predict their detection.

Material and Methods: Twenty-five NCCTs met inclusion criteria of having angiography or MR proven AVM without hemorrhage, prior surgery, or other CNS disease. Demographic variables, clinical symptoms at presentation, abnormal CT imaging findings, attenuation of the superior sagittal sinus (SSS), and Spetzler-Martin grade of each AVM were recorded. We examined the relationship between AVM detection and SSS attenuation through Kruskal–Wallis test. Exploratory serial logistic principal components analysis was performed including demographics, symptoms, and CT features in the multivariate model.

Results: About 80% of the NCCTs showed an abnormality while 20% were normal. All those with an identifiable abnormality showed hyperdensity (80%). Logistic regression models indicate that clustered associations between several CT features, primarily calcifications, hyperdensity, and vascular prominence significantly predicted Spetzler-Martin grade (likelihood ratio 7.7, $P = 0.006$). SSS attenuation was significantly lower in subjects with occult AVMs when compared to those with CT abnormalities (median 47 vs. 55 HU, $P < 0.04$).

Conclusion: Abnormal hyperdensity was evident in all detectable cases (80%) and multiple CT features were predictive of a higher Spetzler-Martin AVM grade. Moreover, SSS attenuation less than 50 HU was significantly correlated with a false-negative NCCT.

Keywords: Arteriovenous malformation, Computed tomography, Neuroradiology

INTRODUCTION

While cerebral arteriovenous malformations (AVMs) occur in only 0.1% of the population,[1] they underlie 1–2% of all strokes, 3% of strokes in young adults, and 9% of subarachnoid hemorrhages.[2] Patients with AVMs can present with wide variations in symptoms that contribute to the difficulty with their diagnosis. Acute symptoms usually arise from a new hemorrhage,

but seizures, headache, and focal neurologic deficits[2,3] can occur without hemorrhage. A recent meta-analysis has shown that AVMs have an overall annual hemorrhage rate of 3%[4] and prior retrospective studies demonstrated that the average annual mortality in patients with untreated brain AVMs ranged from 0.7 to 1.0%.[5,6] While AVMs that previously ruptured have a higher annual rupture rate (4.5%), unruptured AVMs have an annual rupture rate of 1–2%.[4,7]

It is for these reasons that the detection of unruptured AVMs is essential since there are currently many available treatment options that include medical management, microsurgical resection, endovascular embolization, stereotactic radiosurgery, or some combination of these strategies. Early detection is valuable before hemorrhage since AVMs frequently appear in young patients, and in most cases, treatment will provide a complete cure or diminish the likelihood of hemorrhage and its associated morbidity and mortality.[8]

Approximately half of AVMs present with intracranial hemorrhage,[4,7] which is usually first detected with a multidetector non-contrast computed tomography (NCCT) of the head, as this modality has a greater than 90% sensitivity for acute subarachnoid hemorrhage and hemorrhagic stroke.[9-11] Although Almandoz *et al*. have shown that NCCT features along with clinical features in patients presenting with intraparenchymal hemorrhage can establish the probability of an underlying vascular anomaly,[12] the diagnosis of an AVM itself is usually not established on the basis of imaging findings on the non-contrast scan. Whenever there is a reasonably high probability of an underlying vascular lesion, based on age, history, and location of the hemorrhage, the patient should have an MR, MRA, CTA, or digital subtraction cerebral angiography (DSA) for diagnosis.[12]

AVMs usually have a moderately well-defined cluster of closely spaced vascular structures, called the nidus, that, in some cases, will be visible on cross-sectional imaging. While modern CT and MR provide exceptional spatial resolution, the definitive diagnosis of an AVM usually requires the temporal resolution of DSA since the critical diagnostic finding of an AVM is not only a nidus but also the appearance of a contrast within a vein during the arterial phase of injection. This is referred to as the "early vein."[13]

While imagers have come to expect that unruptured AVMs will be difficult or impossible to detect on NCCT, there are much older studies (>30 years ago) that describe some imaging characteristics and very little in the recent literature that quantifies the likelihood of their detection [Table 1]. Since the utilization of NCCTs in the emergency setting has been increasing in the past several decades,[14,15] approximately doubling over a 10-year period,[16] and advances in CT technology during this time have significantly improved; it seems essential for clinicians to be very familiar with the expected NCCT findings of unruptured AVMs. The dearth of recent literature describing and characterizing the NCCT characteristics of this entity and their infrequent occurrence in the course of routine clinical imaging represents a barrier to their recognition without hemorrhage. This study was initiated after one author's experience with an AVM that was prospectively identified on NCCT in a young adult with new seizures, but only by its subtle high attenuation and associated parenchymal calcifications [Figure 1].

On that basis, we performed a retrospective review of patients at two academic hospitals with DSA, CTA, or MR proven unruptured AVMs along with NCCT to determine the likelihood of detection during this modern era of multidetector CT. Our goals in collecting this information were to determine: (1) If advances in CT technology have improved the likelihood of visualization of AVMs on NCCT and (2) establish what specific imaging features contribute to making unruptured AVMs apparent or inapparent on NCCT.

MATERIAL AND METHODS

Center 1

After IRB approval, a retrospective search was performed through this institution's database of reports of cervicocerebral DSA from January 2002 until December 2017. We searched for reports with keywords "AVM," "arteriovenous malformation," and "head" and also without terms "ICH," "rupture," and "hemorrhage." This revealed a total of 106 separate examination reports. Of these 106 examination reports, only patients with available NCCT predating the cerebral angiogram were included in the study. All patients with diagnoses other than AVM (e.g., dural AVF or cavernous-carotid fistula), prior neurosurgery, or intracranial hemorrhage in the general region of the AVM were excluded from the study. From that initial search, 16 patients with unruptured AVMs and NCCT were included in our analysis from Center 1. The diagnosis of AVM was established with DSA in 15 cases and CTA in one.

Center 2

After IRB approval, a retrospective search through this institution's database from March 2019 to November 2019 was performed. We searched reports for "AVM," which resulted in 230 separate reports of initial and follow-up studies performed on patients during the specified time period. These 230 reports and images were reviewed for initial NCCT of the head performed on patients with unruptured AVMs, which spanned a time period of January 2003–March 2019. All studies with alternate diagnosis (e.g., dural AVF or cavernous-carotid fistula), prior neurosurgery,

Table 1: Summary of published literature on NCCT detection of unruptured AVMs.

Year	Author	Patients with NCCT (*n*)	NCCT abnormality detected (*n*)	No NCCT abnormality detected (*n*)	Details	Additional information
1979	Leblanc *et al.*[19]	22	16	6	13 with high or low attenuation lesions 3 with other nonspecific abnormalities	54 total studies evaluated included ruptured AVMs.
1984	Kumar *et al.*[21]	60	50	10	35 with calcifications 36 with intrinsic hypodensities 2 with extrinsic surrounding hypodensity (edema) 33 with mass effect 15 with ectasia of ipsilateral cistern 12 with compression of high convexity sulci	All large unruptured AVMs No specific mention of frequency of cases with NCCT evidence of hyperdensity other than calcifications Vascular prominence was evaluated on contrast enhanced CT
1987	Leblanc *et al.*[20]	13	6	7	1 with calcification 3 with mixed, low, or high attenuation abnormalities	MRI detected AVM in all cases

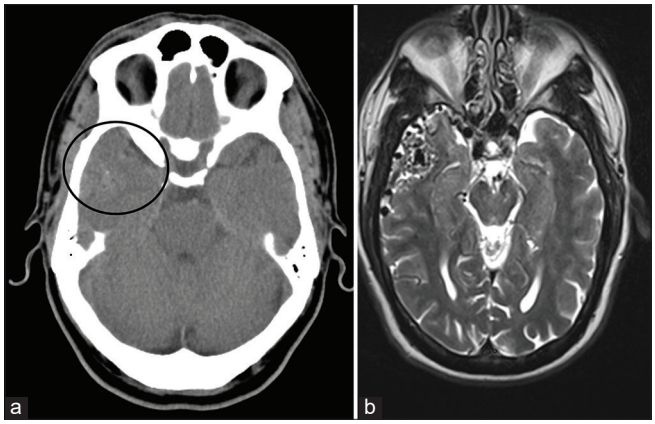

Figure 1: (a and b) Non-contrast CT showing vague hyperattenuation and few calcifications in the right temporal lobe (circle, a). The T2-weighted MR scan at the same level (b) reveals multiple flow voids consistent with intravoxel dephasing from high-velocity flow in the nidus and dilated vasculature of this AVM that was proven on DSA based on arteriovenous shunting.

or intracranial hemorrhage in the location of the AVM were also excluded from the study. This search resulted in nine unruptured AVMs with CT. The diagnosis of AVM was established with DSA in six and typical findings on MR and CTA/MRA in the other three.

Data collection

Numerous clinical variables for each patient were recorded, including demographic variables of age and gender as well as presenting symptomology including presence of headache, seizure, vertigo, visual disturbances, or sensorimotor disturbances [Table 2].

Table 2: Demographics and clinical features of the sample.

Demographics	Center 1		Center 2		Total	
n	16		9		25	
Age (years)	47.4 (16.3)		44.0 (23.5)		46.2 (18.8)	
Gender	12 M	(75%)	7 M	(78%)	19 M	(76%)
	4 F	(25%)	2 F	(22%)	6 F	(24%)
Clinical features						
Headache	5	(31%)	5	(56%)	10	(40%)
Seizure	8	(50%)	2	(22%)	10	(40%)
Vertigo	1	(6%)	0	(0%)	1	(4%)
Visual disturbances	2	(13%)	0	(0%)	2	(8%)
Sensorimotor disturbances	0	(0%)	1	(11%)	1	(4%)

The NCCT images along with subsequent diagnostic vascular imaging of each case were reviewed independently by two investigators to rate the appearance of typical AVM imaging characteristics which included focal high attenuation, calcifications, vascular prominence, parenchymal edema, and adjacent bony change. In addition, the density of the superior sagittal sinus (SSS) in Hounsfield units (HU) was measured in the mid-sagittal sinus using available PACS tools for each case. The investigators then corroborated the location of the abnormalities on each CT with the location of the AVM based on vascular imaging (DSA, CTA, or MRI/MRA) and recorded the Spetzler-Martin grade of each AVM.[17] The independent assessments of the two investigators were recorded and any differences were then reviewed by a third, more senior investigator (CAQ neuroradiologist with 27 years of experience) and resolved [Table 3]. Evidence of abnormality detection in the original interpreting radiologist's report was also recorded.

Table 3: Summary of imaging features.

Non-contrast CT features		Advanced imaging features	
Any abnormality	20 (80%)	Spetzler-Martin grade	
Calcifications	9 (36%)	Grade 1	9 (36%)
Hyperdensity	20 (80%)	Grade 2	8 (32%)
Vascular prominence	14 (56%)	Grade 3	7 (28%)
Parenchymal edema	3 (12%)	Grade 4	1 (4%)
Adjacent bony change	1 (4%)		
SSS density (HU)	57.8 (11.0)		

Data analysis

Data were imported into the R statistical environment for cleaning and analysis.[18] Following assessment of data integrity, descriptive statistics characterizing frequencies of individual clinical and imaging features were first performed. To identify relationships between clinical symptoms, tetrachoric correlations were then calculated. Because we hypothesized that decreased attenuation of the blood pool may influence AVM detectability, we examined the relationship between AVM-positive CT and SSS attenuation through Kruskal–Wallis test.

We also wished to explore the predictive relationships of both clinical and CT imaging data on advanced imaging features; however, traditional analytic options were statistically limited by sample size and associated concerns for multiple testing. Thus, we performed an exploratory logistic principal components analysis (PCA) including demographic (sex and age), presenting symptoms (headache, seizure, vertigo, visual, and sensorimotor), and CT findings (calcifications, hyperdensity, vascular prominence, bony changes, edema, and SSS density) as features in the multivariate model. PCA reduces the dimensionality of the data, maximizing variance explained by the fewest number of orthogonal factors. Logistic PCA is similar to traditional PCA but is specifically designed for the analysis of dichotomous measures; this was ideal given that 11 of our 13 variables were binary. For this analysis and based on natural divisions in the data, age was binarized with a threshold of 45 years, and SSS density was set at a threshold of 70 HU.

Serial logistic PCA was subsequently performed with a range of 1–10 components; a three-factor solution was selected based on a natural elbow in the scree plot. This three-component model explained >70% of the deviance in the data. Factor loadings from the best fit model were examined, and natural groupings in the data were identified. Each of the three principal components was tested for its ability to predict Spetzler-Martin grade through ordinal logistic regression. Specifically, we included all three principal components in the full model and serially attempted to remove individual components. Statistical significance was assessed through likelihood ratio test.

Finally, we assessed the associations between our two continuous measures (age and SSS density) and AVM grade through ordinal logistic regression, after adjusting for other demographic and clinical features. An a of 0.05 (after Bonferroni correction) was selected as the threshold for statistical significance.

RESULTS

[Table 2] summarizes the clinical features of the sample. Our two separate centers' retrospective analyses identified 25 patients with NCCT of brain and proven unruptured AVMs. Of the patients identified, 19 (76%) were male and 6 (24%) were female with a mean age of 46.2 ± 18.8 years. The most common presenting symptoms were seizure and headache (80% of all cases), with seizure more common at Center 1 and headache more common at Center 2. This may be a consequence of the relatively small sample size from each institution. Less frequent symptoms included vertigo, visual symptoms, and sensorimotor symptoms. [Table 4] summarizes correlational patterns between clinical features. Seizure at presentation was more common in males, while headaches were more common in females. Most other presenting symptoms were uncorrelated, although there were modest positive associations between visual symptoms, vertigo, and sensorimotor symptoms.

Of the patients with AVMs that met our inclusion criteria, 80% (20/25) of the AVMs showed some type of abnormality on CT [Figures 2-5], while 20% (5/25) were completely unidentifiable [Figure 6]. We then confirmed that these five were completely unidentifiable on NCCT through additional corroboration with the original interpreting radiologists' report. The attenuation of the SSS was significantly lower in subjects with CT occult AVM (median 47 vs. 55 HU, $c^2 = 4.3$, df = 1, $P = 0.038$). Of those with evident abnormalities on CT, all had some variation of high attenuation in the region of the AVM (20/20) ranging from ill-defined to serpiginous density, while 70% of these also had abnormal vascular prominence (14/20). About 45% of cases (9/20) also demonstrated abnormal calcifications in the region of high attenuation. Low attenuation suggesting edema or encephalomalacia was only seen in 20% (4/20) of the cases, and adjacent bony changes were seen in a single case (5%). In the five cases with no abnormalities to suggest an AVM, there were no other abnormalities elsewhere in the brain or skull.

Only one case demonstrated four CT features of an AVM, that is, focal high attenuation, vascular prominence, calcifications, and adjacent bony change. This case proved to be the only Spetzler-Martin Grade 4 AVM in the sample. There were no Spetzler-Martin Grade 5 AVMs nor micro-AVMs among our cases.

Table 4: Tetrachoric correlations between clinical variables.

	Sex	Headache	Seizure	Vertigo	Visual	Sensorimotor
Sex	1.00					
Headache	–0.75	1.00				
Seizure	0.69	–0.75	1.00			
Vertigo	–0.12	–0.09	–0.09	1.00		
Visual	–0.38	0.14	0.14	0.44	1.00	
Sensorimotor	–0.12	0.32	–0.09	0.59	0.44	1.00

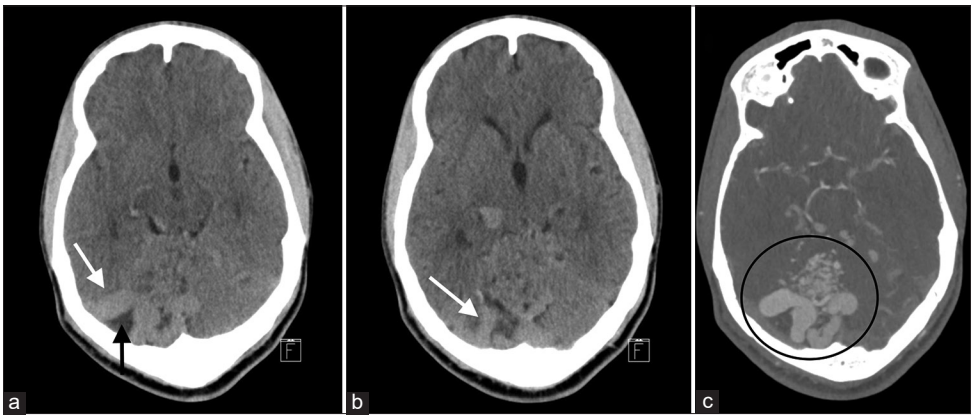

Figure 2: (a-c) Non-contrast CT images demonstrate an AVM with multiple areas of high attenuation within the brain (white arrow, a and b), many of which are sharply defined and serpiginous. The conspicuity of these structures reflects the expected higher than brain attenuation of normal blood within enlarged blood vessels. Additional regions of hypoattenuation surrounding these vessels may indicate edema or encephalomalacia (black arrow, a). The CTA at the same level shows corresponding abnormal vascular structures characteristic of an AVM (circle, c).

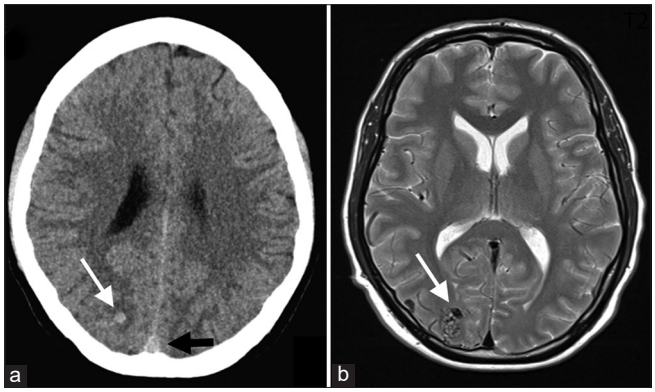

Figure 3: (a and b) Non-contrast CT image demonstrates a focal area of high attenuation (white arrow, a) in the parietal white matter without calcifications or adjacent low attenuation. While hemorrhage is a consideration, note how its attenuation resembles that of the intravascular blood in the superior sagittal sinus (black arrow). This observation broadens the differential to include an abnormal vascular structure, in these cases, small AVMs, as well as hemorrhage and cavernoma. The T2-weighted MR scan at the same level (b) reveals multiple flow voids consistent with intravoxel dephasing from high-velocity flow in the nidus of this small AVM that was proven on DSA based on arteriovenous shunting.

Nine cases demonstrated three abnormal CT features. Seven of these nine showed hyperdensity, vascular prominence, and calcifications [Figure 5]. All seven were Spetzler-Martin Grade 2 and above. One among the nine showed hyperdensity, vascular prominence, and edema and another showed hyperdensity, calcifications, and edema. Seven cases demonstrated two abnormal CT features, five of which

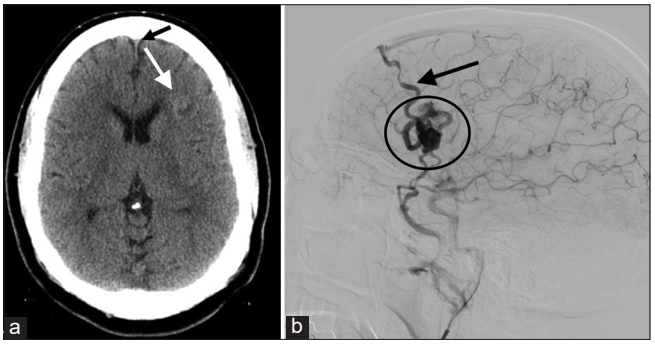

Figure 4: (a and b) Non-contrast CT image shows a subtle abnormality with asymmetric high attenuation in the left frontal lobe white matter (white arrow, a). While hemorrhage is again a consideration, note how its attenuation resembles that of the intravascular blood in the superior sagittal sinus (small black arrow, a). The corresponding DSA (b) demonstrates typical features of an AVM. Note the nidus (circle, b) and early appearance of a superficial vein (black arrow, b) draining into the superior sagittal sinus during the arterial phase of injection into the patient's left carotid artery.

showed hyperdensity and vascular prominence, and the other two showed hyperdensity and edema. Only three cases showed focal high attenuation as the only abnormality, and all of these proved to be Grade 1 AVMs.

Of the five AVMs that were unidentifiable on NCCT, two were Grade 1, two were Grade 2, and one was Grade 3. However, in four of the five cases, the measured attenuation of intravascular blood within the SSS measured 50 HU or less. In the one case with an unidentifiable AVM with attenuation of greater than 50 HU in the SSS, the AVM nidus measured about 1 cm based on dimensions from MR.

Figure 5: This non-contrast CT demonstrates the characteristic appearance of an AVM. Note the curving hyperdense structure (circle) with the same attenuation as the superior sagittal sinus (black arrow). Also note the focal calcification (white arrow). This combination of findings was evident in half of our cases where the AVM was visible on NCCT.

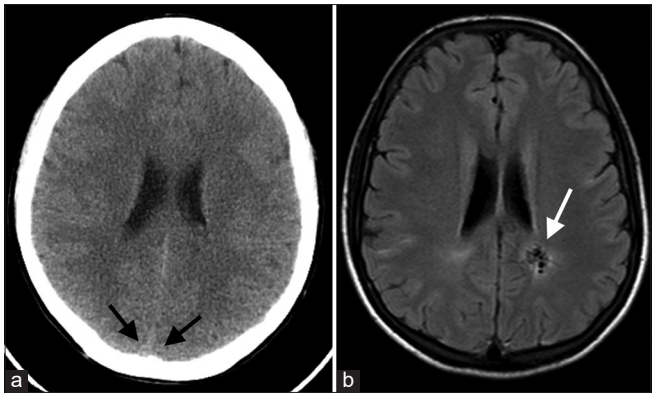

Figure 6: (a and b) This AVM was rated as undetectable on non-contrast CT (a). While the corresponding image from an MR FLAIR sequence demonstrates multiple flow voids consistent with an AVM (white arrow, b), there was no high attenuation from the AVM nidus or supplying vessels visible on CT even in retrospect. But note the low contrast between the brain cortex and superior sagittal sinus (black arrows, a), which measured 49 HU centrally. The low contrast between this patient's intravascular blood and normal brain may contribute to the low conspicuity of this AVM on non-contrast CT.

Results from logistic PCA are summarized in [Figure 7a-c]. The first component (PC1) again identified the relationship between sex and clinical presentation, with males associated with seizures and females with headaches. The second component (PC2) clustered associations between several CT features, primarily calcifications, hyperdensity, and vascular prominence, with a weaker loading on bony changes. The third component primarily identified associations between age and SSS density. Logistic regression models found that PC2 significantly predicted Spetzler-Martin grade (likelihood ratio 7.7, $P = 0.006$), with a progressive increase in PC2 score with increasing AVM grade [Figure 7c]. Associations between AVM grade and the other two principal components were not statistically significant.

We observed an inverse association between SSS density and Spetzler-Martin grade, with lower grades associated with higher density. However, this association was not statistically significant (likelihood ratio 2.1, $P = 0.15$). Patient age was inversely associated with AVM grade (likelihood ratio 8.9, $P = 0.003$), with younger patients generally having higher grade AVMs in our sample.

DISCUSSION

There are a few papers in the imaging literature that mention the conspicuity of AVMs on CT, but these prior studies appeared in the pre-helical CT era. In one review of the CT findings of 54 patients at the Montreal Neurological Institute with AVMs published in 1979, over half (30/54) presented with hemorrhage. Among the 24 cases with unruptured AVMs, 22 cases had CT available for review, six of which were interpreted as entirely normal. 13/22 CT scans demonstrated a high or low attenuation lesions, and the remaining 3/22 scans showed other non-specific abnormalities, such as infarct or dilatation of an ipsilateral ventricle. It is of interest that in six cases included in that study, no AVM was demonstrated on conventional angiography. On that basis, we can assume that some of the lesions detected on CT were cavernomas.[19]

In 1987, the superior sensitivity of MRI for the diagnosis of AVM when compared with CT was reported in 15 patients.[20] Among the 13 patients with NCCT, only a single patient demonstrated visible calcifications, and three had mixed, low, or high attenuation abnormalities. Seven of the 13 scans (53%) were completely normal. An additional, larger study by Kumar *et al*. in 1984 described the non-contrast and contrast-enhanced CT features in 60 unruptured AVMs, and showed a substantially higher NCCT detection rate of abnormalities in 50/60 scans (83%), although this is likely due to inclusion of only large AVMs in this series[21] [Table 1 for additional details].

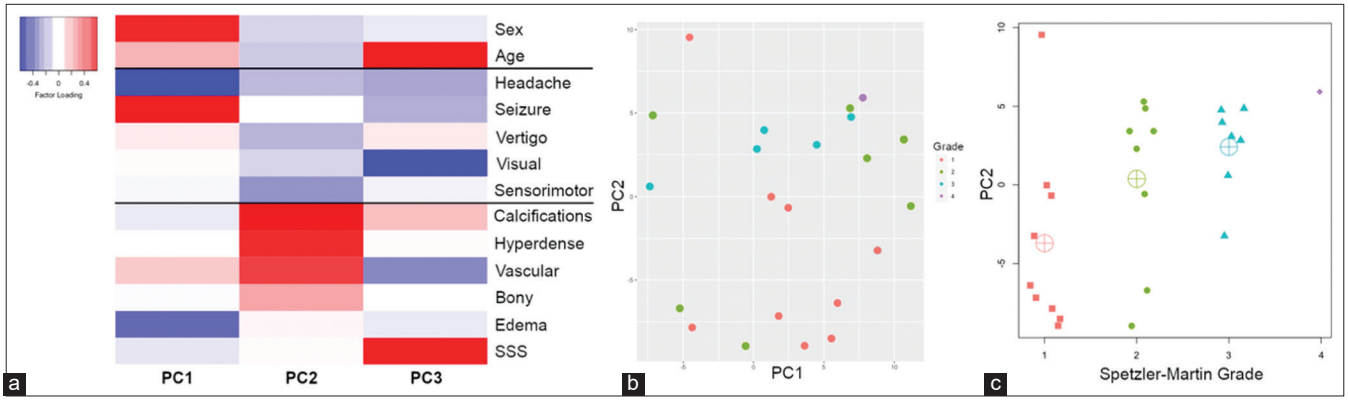

Figure 7: (a-c) Results from logistic PCA. Panel A provides factor loadings for the 3-component solution that included demographic, clinical, and imaging features; this analysis accounted for 71% of the deviance in 13 binary predictors. Panel B is a scatterplot between the two largest principal components, with subjects color coded by Spetzler-Martin grade. Panel C shows the relationships between the component dominated by imaging features (PC2) and Spetzler-Martin grade. Crosshairs represent group means.

The paucity of information in the recent literature on the subject of the detection of AVMs using modern multidetector CT, which has high spatial resolution, may reflect the relatively infrequent detection of unruptured AVMs on NCCTs as well as the tacit acceptance that NCCT is not reliable for their detection. Berman *et al.* suggested in a paper from 2000 that the true prevalence of cerebral AVMs is unknown because they are rare, and the asymptomatic cases may be undercounted.[22] Based on incidence of detection, they predict the prevalence of 10.3 per 100,000. To put this in perspective, one should consider the prevalence of a more common vascular abnormality, cerebral aneurysm, which has a prevalence that is estimated to be 2000 per 100,000 or 2%, that is, 200x higher.[23]

The diagnostic difficulties in identifying AVMs on CT along with their low prevalence, especially those that present without rupture, very likely account for our difficulties in identifying a large number of cases for this study. In a careful search for documented AVM cases with CT from two institutions, we screened 336 radiology reports but found only 25 cases with proven AVMs without clinical or radiologic evidence of hemorrhage.

Based on this carefully selected series, the AVM was visible in some fashion on multidetector helical NCCT in 20/25 cases, with only 20% of scans rated as completely normal. This represents a substantial improvement compared to previously reported CT detection rates and likely reflects the improvement in CT hardware and reconstruction software over the intervening years.

The most common finding, seen in all positive scans, was abnormal high attenuation in the brain reflecting some combination of the nidus and associated supply and draining vessels. In about half of those cases, abnormal brain parenchymal calcifications were also evident. The most common set of findings, evident in about a third of our cases, was parenchymal focal high attenuation, prominent vasculature, and abnormal calcifications.

We did not expect to see evidence of an AVM on NCCT in all of these cases since the detection of small AVMs can be difficult even on DSA. However, we found it of interest that in four of the five cases with no detectable abnormalities on NCCT, the attenuation of intravascular blood, measured in the center of the mid-SSS, was lower than that of blood in this venous sinus in the cases with CT imaging abnormalities. This reached statistical significance even in this relatively small group of patients.

This emphasizes the reason why AVMs are apparent on NCCT. With the exception of calcifications, visualization of the nidus and associated enlarged vessels is entirely due to the fact that normally blood in the intravascular compartment is of higher attenuation than the brain parenchyma. The X-ray attenuation of flowing, intravascular blood has been demonstrated to correlate with the patient's hematocrit, and the ratio of the measured attenuation of blood in the venous sinuses on NCCT with the patient's hematocrit can be used to diagnose venous thrombosis on NCCT.[24,25] Since the detection of abnormal vessels and the AVM nidus on NCCT depends on the intravascular compartment having a higher attenuation than the brain parenchyma, it follows that in patients with low attenuation intravascular blood either from low hemoglobin or hemodilution, the AVM will not be visible on NCCT.

A central limitation of this study is that only cases with proven AVMs were included in this retrospective study of findings on CT. As a result, we can only report the findings in patients with AVMs that were eventually diagnosed. Since only about half of AVMs will lead to hemorrhage and some patients with AVMs are asymptomatic, it is entirely possible that patients with AVMs had NCCT scans during this time period that were read as normal. In addition, while we did

not perform a blinded retrospective review of all 25 scans, our data regarding lack of detection of AVM were also corroborated with the original interpreting radiologists' reports, who in essence were likely "blinded" to the patient's eventual diagnosis of AVM.

It is accepted that CT features in patients with intraparenchymal hemorrhage should be considered along with age and clinical history to predict the likelihood of an underlying vascular anomaly as the cause of hemorrhage and on that basis order vascular imaging.[12] We would add that in patients with the absence of intracranial hemorrhage and an attenuation of intravascular compartment blood similar to brain attenuation, it is likely that an unruptured AVM will be overlooked on NCCT. Just as with the patients with intraparenchymal hemorrhage, these patients may benefit from additional imaging, such as MR with or without MRA, especially when their symptoms could be on the basis of an underlying, unruptured AVM.

CONCLUSION

We found that in 80% of our patients with unruptured AVMs, abnormal high attenuation in the brain, with or without calcification, was evident on CT. This is a higher percentage than reported in early imaging studies with similar inclusion criteria[19,20] and very likely reflects improvements in CT imaging technology. The presence of multiple CT findings including hyperdensity, vascular prominence, and calcifications was significantly predictive of a higher Spetzler-Martin AVM grade. In the five patients with AVMs and scans rated as normal, four of the five had a relatively low attenuation of blood in the SSS (50 HU or less) and the fifth had a small 1 cm AVM. It seems likely that in patients with low contrast between brain parenchyma and the intravascular blood, the AVM nidus and associated vascular structures will be inapparent on NCCT and additional imaging is necessary for detection when an AVM is suspected as the source of symptoms.

Declaration of patient consent

Patient's consent not required as patients identity is not disclosed or compromised.

Financial support and sponsorship

Nil.

Conflicts of interest

There are no conflicts of interest.

REFERENCES

1. Mohr JP, Kejda-Scharler J, Pile-Spellman J. Diagnosis and treatment of arteriovenous malformations. Curr Neurol Neurosci Rep 2013;13:324.
2. Al-Shahi R, Warlow C. A systematic review of the frequency and prognosis of arteriovenous malformations of the brain in adults. Brain 2001;124:1900.
3. Garcin B, Houdart E, Porcher R, Manchon E, Saint-Maurice JP, Bresson D, *et al*. Epileptic seizures at initial presentation in patients with brain arteriovenous malformation. Neurology 2012;78:626.
4. Gross BA, Du R. Natural history of cerebral arteriovenous malformations: A meta-analysis. J Neurosurg 2013;118:437.
5. Brown RD Jr., Wiebers DO, Forbes G, O'Fallon WM, Piepgras DG, Marsh WR, *et al*. The natural history of unruptured intracranial arteriovenous malformations. J Neurosurg 1988;68:352.
6. Ondra SL, Troupp H, George ED, Schwab K. The natural history of symptomatic arteriovenous malformations of the brain: A 24-year follow-up assessment. J Neurosurg 1990;73:387.
7. Lawton MT, Rutledge WC, Kim H, Stapf C, Whitehead KJ, Li DY, *et al*. Brain arteriovenous malformations. Nat Rev Dis Prim 2015;1:15008.
8. Derdeyn CP, Zipfel GJ, Albuquerque FC, Cooke DL, Feldmann E, Sheehan JP, *et al*. Management of brain arteriovenous malformations: A scientific statement for healthcare professionals from the American heart association/ American stroke association. Stroke 2017;48:e200-24.
9. Byyny RL, Mower WR, Shum N, Gabayan GZ, Fang S, Baraff LJ. Sensitivity of noncontrast cranial computed tomography for the emergency department diagnosis of subarachnoid hemorrhage. Ann Emerg Med 2008;51:697-703.
10. McCormack RF, Hutson A. Can computed tomography angiography of the brain replace lumbar puncture in the evaluation of acute-onset headache after a negative noncontrast cranial computed tomography scan? Acad Emerg Med 2010;17:444-51.
11. Brazzelli M, Sandercock PA, Chappell FM, Celani MG, Righetti E, Arestis N, *et al*. Magnetic resonance imaging versus computed tomography for detection of acute vascular lesions in patients presenting with stroke symptoms. Cochrane Database Syst Rev 2009;4:CD007424.
12. Almandoz JE, Schaefer PW, Forero NP, Falla JR, Gonzalez RG, *et al*. Diagnostic accuracy and yield of multidetector CT angiography in the evaluation of spontaneous intraparenchymal cerebral hemorrhage. AJNR Am J Neuroradiol 2009;30:1213-21.
13. Geibprasert S, Pongpech S, Jiarakongmun P, Shroff MM, Armstrong DC, Krings T. Radiologic assessment of brain arteriovenous malformations: What clinicians need to know. Radiographics 2010;30:483-501.
14. Yun BJ, Borczuk P, Zachrison KS, Goldstein JN, Berlyand Y, Raja AS. Utilization of head CT during injury visits to United States emergency departments: 2012-2015. Am J Emerg Med 2018;36:1463-6.
15. Bellolio MF, Heien HC, Sangaralingham LR, Jeffery MM, Campbell RL, Cabrera D, *et al*. Increased computed tomography utilization in the emergency department and its association with hospital admission. West J Emerg Med 2017;18:835-45.

16. Selvarajan SK, Levin DC, Parker L. The increasing use of emergency department imaging in the United States: Is it appropriate? AJR Am J Roentgenol 2019;213:W180-4.
17. Spetzler RF, Martin NA. A proposed grading system for arteriovenous malformations. J Neurosurg 1986;65:476-83.
18. R Core Team. R: A Language and Environment for Statistical Computing. R Foundation for Statistical Computing, Vienna, Austria: R Core Team; 2020.
19. LeBlanc R, Ethier R, Little JR. Computerized tomography findings in arteriovenous malformations of the brain. J Neurosurg 1979;51:765-72.
20. Leblanc R, Levesque M, Comair Y, Ethier R. Magnetic resonance imaging of cerebral arteriovenous malformations. Neurosurgery 1987;21:15-20.
21. Kumar AJ, Fox AJ, Vinuela F, Rosenbaum AE. Revisited old and new CT findings in unruptured larger arteriovenous malformations of the brain. J Comput Assist Tomogr 1984;8:648-55.
22. Berman MF, Sciacca RR, Pile-Spellman J, Stapf C, Connolly ES Jr., Mohr JP, *et al*. The epidemiology of brain arteriovenous malformations. Neurosurgery 2000;47:389-97.
23. Rinkel GJ, Djibuti M, Algra A, van Gijn J. Prevalence and risk of rupture of intracranial aneurysms: A systematic review. Stroke 1998;29:251-6.
24. Buyck P, De Kayzer F, Vanneste G, Wilms G, Thijs V, Demaerel P. CT density measurement and H: H ratio are useful in diagnosing acute cerebral venous sinus thrombosis. AJNR Am J Neuroradiol 2013;34:1568-72.
25. Black D, Rad A, Gray L, Campeau NG, Kallmes DF. Cerebral venous sinus density on noncontrast CT correlates with hematocrit. AJNR Am J Neuroradiol 2011;32:1354-7.

How to cite this article: Mattay RR, Miner L, Copelan AZ, Davtyan K, Schmitt JE, Church EW, *et al*. Unruptured arteriovenous malformations in the multidetector CT era: Frequency of detection and predictable failures. J Clin Imaging Sci 2022;12:5.